NMR IN BIOMEDICINE
NMR Biomed. in press
Published online in Wiley InterScience (www.interscience.wiley.com). DOI:10.1002/nbm.973

Quantification of phosphocholine and glycerophosphocholine with ^{31}P edited ^{1}H NMR spectroscopy

Nikolaus M. Loening,[1]* Anne M. Chamberlin,[1] Andrea G. Zepeda,[2] R. Gilberto Gonzalez[3], and Leo L. Cheng[2,3]

[1]Department of Chemistry, Lewis & Clark College, 0615 SW Palatine Hill Road, Portland, OR 97219, USA
[2]Department of Pathology, Massachusetts General Hospital, Harvard Medical School, Boston, MA 02129, USA
[3]Department of Radiology, Massachusetts General Hospital, Harvard Medical School, Boston, MA 02129, USA

Received 8 December 2003; Revised 15 March 2004, 9 July 2004, 5 April 2005; Accepted 26 May 2005

ABSTRACT: Choline and the related compounds phosphocholine (PC) and glycerophosphocholine (GPC) are considered to be important metabolites in oncology. Past studies have demonstrated correlations linking the relative ratios and concentrations of these metabolites with the development and progression of cancer. Currently, *in vivo* and tissue *ex vivo* magnetic resonance spectroscopy methods have mostly centered on measuring the total concentration of these metabolites and have difficulty in differentiating between them. Here, a new scheme that uses ^{31}P edited ^{1}H spectroscopy to quantify the concentrations of choline, PC and GPC in biological samples is reported and its applicability is demonstrated using samples of human brain tumor extracts. This method is particularly well-suited for analytical situations where the PC and GPC resonances are not sufficiently resolved and/or are obscured by other metabolites. Consequently, this scheme has the potential to be used for the analysis of choline compounds in *ex vivo* tissue samples. Copyright © 2005 John Wiley & Sons, Ltd.

KEYWORDS: ^{31}P edited ^{1}H NMR; INEPT; choline compounds; human brain tumor extracts

INTRODUCTION

Choline and the related compounds phosphocholine (PC) and glycerophosphocholine (GPC) are essential nutrients that function as substrates in many major bio-metabolic pathways. These choline-compounds participate in a number of biological processes ranging from the normal development of the brain and liver in infants[1] to various pathological conditions such as the progression of neoplasm.[2] Although the biochemical functions of these compounds have been studied for decades, their unique importance has only come to light over the past 20 years with the application of NMR spectroscopy to medical science.

The relationship between the concentrations of choline-compounds and pathology has been measured and documented for many medical conditions, such as HIV infections,[3] traumatic brain injuries,[4] schizophrenia,[5] neuro-degenerative[6] and neuro-genetic[7] disorders, chronic fatigue[8] and multiple sclerosis,[9] as well as for the processes of normal development[10] and aging.[11] However, one of the most studied connections has been with cancer.[12–18] In general, the concentrations of choline-compounds are elevated in cancer and, more importantly, *ex vivo* studies of tissue extract samples suggest that the ratio of the phosphoryl derivatives indicates the status of the disease.[19–21] The signals of the methyl [$-N(CH_3)_3$] protons has been used to differentiate choline (3.185 ppm) from PC (3.208 ppm) and GPC (3.212 ppm) in *ex vivo* analyses.[22] Unfortunately, present NMR-based *in vivo* techniques cannot differentiate the methyl protons of choline from those of PC and GPC as their signals are separated by less than 0.03 ppm. For *ex vivo* samples of intact tissue the methyl protons of choline can be differentiated from those of the other choline compounds using high-resolution magic angle spinning proton NMR spectroscopy. Differentiating between the methyl protons of PC and GPC is a great challenge because of their very small chemical shift separation (0.007 ppm, see Results section).[23,24] Therefore, even at moderate field strengths (e.g. 300 MHz), the resonances are difficult to resolve. This means that it is currently almost impossible to quantify these metabolites simultaneously *in vivo*. Although *ex vivo* quantification of all three compounds

**Correspondence to:* N. M. Loening, Department of Chemistry, Lewis & Clark College, 0615 SW Palatine Hill Road, Portland, OR 97219, USA.
E-mail:
Contract/grant sponsor: NIH; *contract/grant number:* F32 NS42425-01.
Contract/grant sponsors: Camille and Henry Dreyfus Foundation; NIH NIBIB; *contract/grant number:* EB002026.
Contract/grant sponsor: NIH NCI; *contract/grant numbers:* CA77727, CA095624, CA83159.

Abbreviations used: GPC, glycerophosphocholine; INEPT, insensitive nuclei enhanced by polarization transfer; PC, phosphocholine.

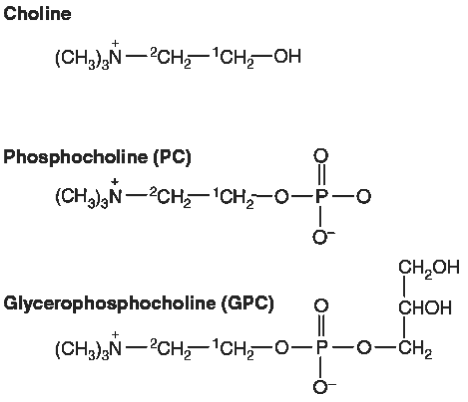

Figure 1. Molecular structures of choline, PC, and GPC. The ^{31}P edited ^{1}H experiment discussed in the text uses INEPT steps to transfer magnetization from the $^{1}CH_2$ protons to the phosphorous nuclei and back, and selectively refocuses the scalar couplings between the $^{1}CH_2$ and $^{2}CH_2$ protons during the transfers

is possible using the methyl proton signals, it is difficult and requires techniques such as post-processing peak deconvolution or two-dimensional spectroscopy.[25–28]

Here, we introduce a scheme that can efficiently differentiate and quantify PC and GPC, and we demonstrate its applicability to both model compounds and extracts of human brain tissue. The crux of this method is the use of phosphorous (^{31}P) edited proton (^{1}H) NMR spectroscopy to measure signals from the $^{1}CH_2$ protons (see Fig. 1) of PC and GPC. These protons have a spectral separation that is about 20 times greater than that between the methyl protons (0.13 vs 0.007 ppm). The ^{31}P editing is accomplished using the scalar couplings between the ^{31}P nucleus and the $^{1}CH_2$ protons in PC and GPC. Although the sensitivity of this technique suffers compared with the direct analysis of the methyl protons, the better resolution of the $^{1}CH_2$ protons allows for analysis in situations where the individual methyl proton resonances from the three choline compounds are not sufficiently resolved. Consequently, we believe this approach may be helpful in the future for *ex vivo* analyses of intact tissue samples and, if sensitivity issues can be resolved, has the potential to be incorporated into *in vivo* examinations.

EXPERIMENTAL

The experiments were carried out using vertical standard-bore Bruker Avance NMR spectrometers. The standard samples were studied using a 300 MHz (7.05 T) system equipped with a Bruker broadband inverse-geometry *z*-axis gradient probe. The brain tissue extract samples were studied using a 600 MHz (14.1 T) system equipped with a Bruker ^{31}P/^{13}C/^{15}N–^{1}H inverse-geometry *z*-axis gradient probe. The pulse sequence developed for the experiment is shown in Fig. 2. It consists of two INEPT steps[29] that transfer the initial ^{1}H magnetization to ^{31}P and then back to ^{1}H. Inserted into these INEPT steps are selective 180° pulses that only affect the $^{2}CH_2$ protons and, consequently, refocus the homonuclear scalar couplings between the $^{1}CH_2$ and $^{2}CH_2$ protons. These selective pulses are essential because the ^{1}H–^{1}H couplings are similar in size to the ^{31}P–^{1}H couplings. Without the selective pulses the effect of the ^{1}H–^{1}H couplings during the INEPT delays would be to transform the single quantum coherences arising from the $^{1}CH_2$ protons into multiple quantum coherences. Pulsed field gradients are used in conjunction with phase cycling to eliminate unwanted signals in the ^{31}P edited ^{1}H spectra. The gradients G_1 and G_2 impart a phase label to the ^{31}P magnetization that is later refocused after the magnetization has been transferred to ^{1}H by the final coherence selection gradient, G_3. Finally, a zero-quantum filter is included at the end of the sequence to further attenuate contributions from undesired coherence transfer pathways.[30]

A recycle time of 10 s was used for both the regular and ^{31}P edited experiments to ensure that the sample magnetization was at equilibrium before every scan. During the

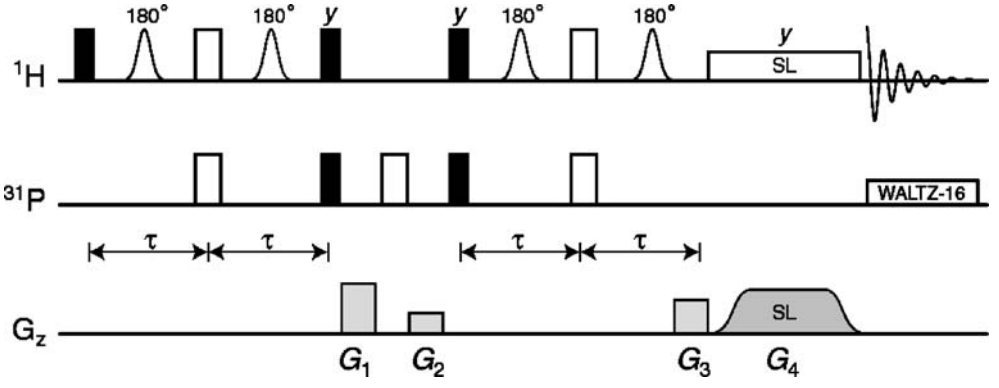

Figure 2. The pulse sequence used to acquire the ^{31}P edited ^{1}H spectra. For the ^{1}H and ^{31}P channels, solid rectangles correspond to 90° radiofrequency pulses, open rectangles correspond to 180° pulses, and Gaussian shapes represent selective 180° pulses. The spin-lock pulse is denoted by 'SL'. The phase of all pulses is *x* unless indicated otherwise

recycle delay, the water resonance was saturated with a weak radio frequency field ($\gamma B_1/2\pi = 50$ Hz). Low power Waltz-16 decoupling[31] ($\gamma B_1/2\pi = 625$ Hz) was used on the ^{31}P channel during ^{1}H acquisition to narrow the lines of the PC and GPC $^{1}CH_2$ resonances; this resulted in an increase (20%) in the sensitivity of the experiment. For the high-power pulses, the radiofrequency field strength ($\gamma B_1/2\pi$) was 40 kHz for ^{1}H and 10 kHz for ^{31}P on the 14 T instrument, and 35 kHz for ^{1}H and 20 kHz for ^{31}P on the 7 T instrument. For the ^{31}P experiments, Waltz-16 decoupling ($\gamma B_1/2\pi = 2500$ Hz) was used on the ^{1}H channel.

In the ^{31}P edited ^{1}H experiment, Gaussian 180° pulses were used to selectively decouple the ^{1}H homonuclear scalar couplings during the INEPT steps. The selective pulses were 5 ms on the 14 T system and 10 ms on the 7 T system; for both systems the pulses were applied at 3.3 ppm. Consequently, these pulses refocused the $^{2}CH_2$ protons of choline, PC, and GPC, but left the $^{1}CH_2$ protons of these molecules unperturbed. The gradients G_1, G_2, G_3 and G_4 were set to 35, 15, 20, and 1 G cm^{-1} and were 2.47, 2.47, 1, and 10 ms in length, respectively. The first three gradients were shaped to a half-sine bell; the shape of the fourth gradient was constant over the central 80% of the pulse and was smoothly ramped on and off at the ends of the pulse.

The sample temperature was maintained at 10 °C with a cooling gas flow rate of 535 l h^{-1} for the experiments at 14 T to minimize any potential problems owing to sample degradation. The experiments at 7 T were performed at 25 °C. The temperature was controlled to better than ± 0.2 °C during the experiments; temperature stability is important for quantitation as the efficiency of the heteronuclear transfer steps varies with temperature.

Standards

The standard samples consisted of between 0 and 5 mM PC, between 0 and 5 mM GPC, and 3.1 mM choline in 10% D_2O–90% H_2O. D_2O was included in the sample for the purpose of locking the magnet field. All spectra for the standards were acquired with 16 scans (each spectrum required just under 3 min to complete). The pH of each sample was adjusted to be in the range 6–7.5 by the addition of small amounts of HCl or NaOH.

Solutions of human brain tumor metabolites

Eleven samples of human glioma (malignant brain tumor) extracts were prepared using the FastPrep™ and Speed Vac® systems (Thermo Savant, Holbrook, NY, USA) according to the following procedure. Between 100 and 200 mg of frozen tissue samples from surgeries or autopsies were transferred into Lysing Matrix D tubes (Qbiogene, Carlsbad, CA, USA) along with 1.2 ml methanol. The sample tubes were then placed in the FastPrep™ system and processed for 35 s on speed dial 4.0. This was repeated at least three times until no visible tissue pieces remained. Next, a modified methanol–chloroform extraction was carried out.[32] The resulting aqueous layer of brain metabolites was dried with the Speed Vac® system and redissolved in D_2O. The pH of these samples was adjusted to be in the range 7–8. Since this preparation method is not a calibrated protocol for metabolite quantification, we observed a decrease in the absolute metabolite concentrations. For instance, the mean concentration for total choline was determined to be 0.31 ± 0.07 mM, which is only 25% of the literature values (1.24 ± 0.10 mM) for extracts of tumor tissues of similar type.[33–35] Although this reduction in concentration resulted in much longer experiment times, it did not interfere with the aim of this work, which was to test the capability of the ^{31}P edited ^{1}H spectral protocol to quantify PC and GPC concentrations of tissue extract samples. ^{1}H spectra for the brain extracts were acquired using 1024 scans, resulting in an experiment time of 3.2 h. ^{31}P edited ^{1}H spectra were acquired using between 3096 and 5192 scans, resulting in experiment times ranging from 9.8 to 16.3 h.

RESULTS

^{31}P edited spectra of the standards

The method described in this report concentrates on the measurement of signals from the $^{1}CH_2$ protons instead of the more intense signals that arise from the methyl protons. Focusing on the $^{1}CH_2$ protons has two main advantages. First, as seen in the regular ^{1}H spectrum shown in Fig. 3(a), the signals from the $^{1}CH_2$ protons are dispersed over a range of 0.13 ppm instead of the 0.007 ppm range of the methyl protons. This suggests that the measurement of the $^{1}CH_2$ protons is better suited for situations, such as *ex vivo* tissue analyses, where the spectral resolution is limited to the point that the individual methyl resonances cannot be resolved. The second advantage is that the $^{1}CH_2$ protons for PC and GPC have observable ($\sim$6.1 and 6.3 Hz, respectively [22]) couplings to the ^{31}P nucleus, which allows for the use of ^{31}P editing. This fact is important as, without ^{31}P editing, the ^{1}H signals of the choline-compounds (especially those from the $^{1}CH_2$ resonances but also the methyl resonances) are mingled with signals from other metabolites, making quantification more difficult and less reliable.

The main disadvantage of our method is that the integral of the $^{1}CH_2$ protons is 4.5 times smaller than the integral of the methyl protons [note the separate intensity scale used for the methyl region in Fig. 3(a)]. Nevertheless, the quality of the ^{31}P editing allows the relatively weak $^{1}CH_2$ peaks to be easily resolved and measured in a ^{31}P edited ^{1}H spectrum. With ^{31}P editing,

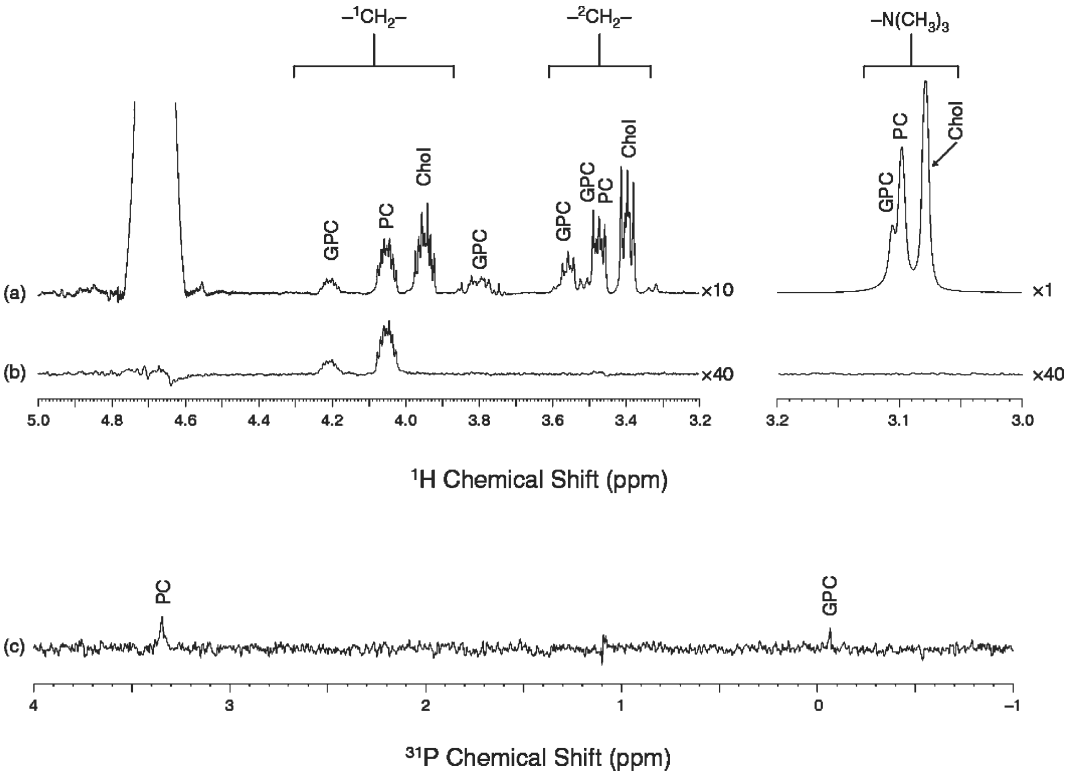

Figure 3. (a) ^{1}H, (b) ^{31}P filtered ^{1}H, and (c) ^{31}P spectra for a standard sample of 3.1 mM choline, 2.0 mM PC, and 1.0 mM GPC in 10% D_2O–90% H_2O. Each spectrum was acquired in 16 scans and with heteronuclear decoupling at 300 MHz for ^{1}H. The lack of resolution in the methyl region (3.12–3.06 ppm) is what makes it hard to use the methyl peaks to quantify the concentrations of choline, PC, and GPC in tissue samples. In spectrum (a), the additional GPC peaks at 3.78 ppm and overlapping the $^2CH_2$ resonances at 3.5 ppm arise from the glycerol moiety. The relative scales for spectra (a) and (b) are indicated at the right of each part. All spectra were processed with 0.5 Hz of line broadening; baseline correction was used for spectrum (a) to compensate for the intense water signal at 4.7 ppm

the only peaks that remain in the ^{1}H spectrum are those from the $^1CH_2$ protons of PC and GPC. The signal from the $^1CH_2$ protons of choline, which would have appeared at 3.95 ppm, is completely removed, as are the intense methyl signals at ~3.1 ppm from all three choline compounds. The small artifact at 4.7 ppm in the ^{31}P edited ^{1}H spectrum is all that remains of the water signal after suppression by presaturation and coherence transfer pathway selection. This artifact has an integral close to zero and is 0.5 ppm downfield from the signals of interest, so it does not affect the integration of the GPC and PC signals.

Signals from choline are removed in the ^{31}P editing step, so it is not possible to determine its concentration directly from the ^{31}P edited ^{1}H spectrum. However, the quantitative relationship between the ^{31}P edited and the regular ^{1}H spectra can be exploited to determine the choline concentration. This can be accomplished by determining the PC and GPC concentrations from the edited spectrum, and then using this information to subtract their contributions from the total integrated intensity of the methyl protons in the regular ^{1}H spectrum. The remaining intensity corresponds to the concentration of choline. As a result, it is possible to determine the relative concentrations of all three species in cases where the individual methyl signals are not resolved.

Quantification of the amount of choline, PC, and GPC in a sample using ^{31}P edited ^{1}H spectra depends on the transfer efficiency of the INEPT steps. This transfer efficiency, in turn, depends on the ^{31}P–^{1}H coupling constants, pulse imperfections, and the transverse and longitudinal relaxation rates. The coupling constants are largely insensitive to sample conditions and the INEPT steps are reasonably tolerant of variations in pulse calibration, so the main difficulty with establishing the transfer efficiency stems from variations in the relaxation rates. For the range of concentrations used in our samples we found that the transfer efficiencies were independent of the relative concentrations of choline, PC, and GPC. However, relaxation rates (and therefore the transfer efficiency) depend on temperature so it is important to establish the transfer efficiency for whatever temperature is used for the experiment. For our experiments with brain tissue samples, which were kept at 10 °C, we observed signal intensities in the ^{31}P edited spectra that were 13.4 and 18.5% of the unedited signal intensities for

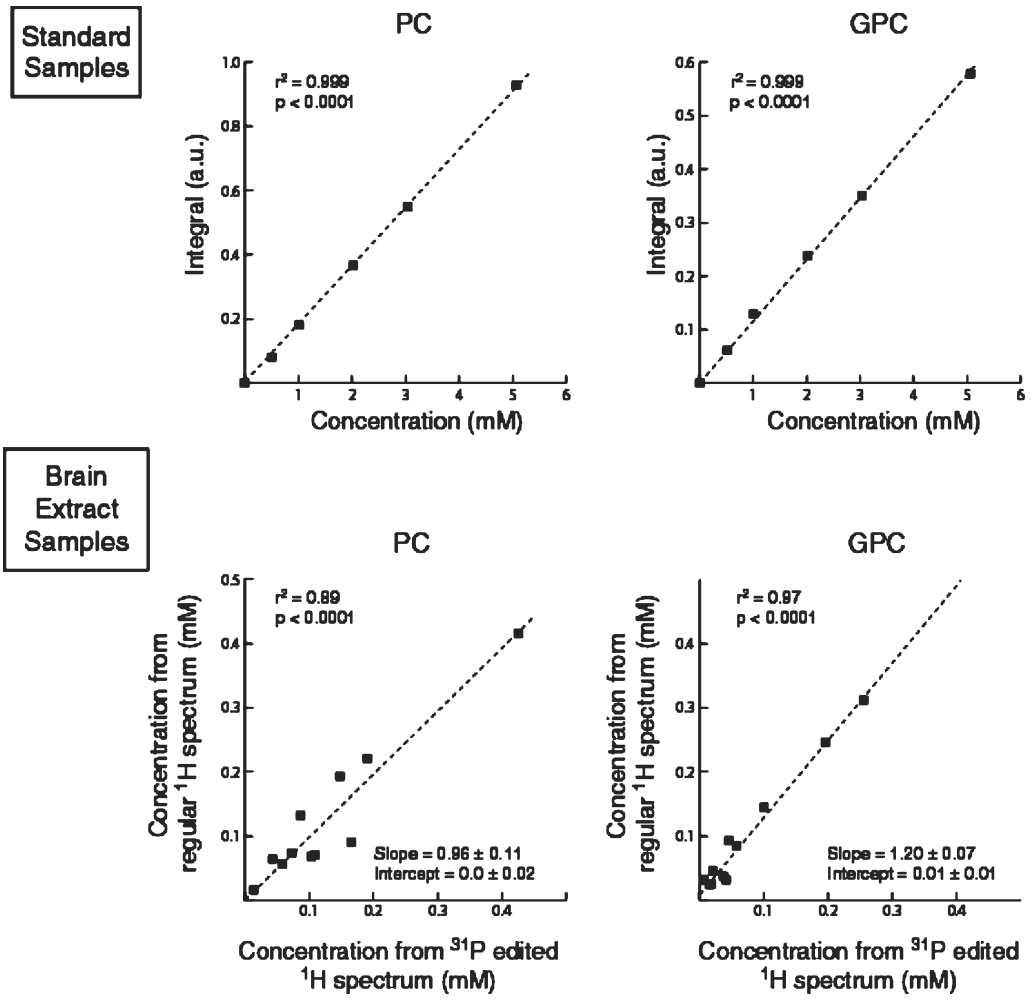

Figure 4. At the top are graphs demonstrating the linear response of the integrals from $^{1}CH_2$ peaks in the ^{31}P edited H spectra for the standard samples (0–5 mM PC, 0–5 mM GPC and 3.1 mM choline in 10% D_2O–90% H_2O) at 300 MHz. At the bottom are graphs showing how the concentrations of PC and GPC, determined by fitting the methyl peaks in regular ^{1}H spectra, compare with the concentrations determined using the integrals of the $^{1}CH_2$ peaks in the ^{31}P edited ^{1}H spectra. These results were determined from spectra acquired at 600 MHz for ^{1}H for the brain extract samples described in the text. The dotted lines indicate the results from linear regression analyses of the data; the result of each analysis is shown with the relevant graph

PC and GPC, respectively. These results are 54 and 74% of the theoretical maximum transfer efficiency of 25% (see Discussion section). At 25 °C, the transfer efficiencies (PC = 24.1% and GPC = 20.1%) were much closer to the theoretical value, as would be expected based on the connection between temperature and relaxation rates for small molecules in solution.

The top half of Fig. 4 demonstrates the linear relationship between the PC and GPC peak integrals in the ^{31}P edited ^{1}H spectra and the PC and GPC concentrations for a series of standard samples.

Analyses of human brain extracts

We tested the applicability of ^{31}P editing for the quantification of PC and GPC in biological systems using a series of 11 human glioma extract samples. Representative 600 MHz ^{1}H spectra for one of these samples are shown in Fig. 5. From the subspectrum shown in Fig. 5(b), it is clear that the $^{1}CH_2$ resonances are overlapped by peaks from other metabolites in the regular ^{1}H spectrum; this problem also affects the methyl resonances, although to a smaller extent. The complexity of the spectrum makes it difficult to quantify the relative amounts of the choline compounds using just the regular ^{1}H spectrum.

In the ^{31}P edited ^{1}H spectrum [Fig. 5(c)], the $^{1}CH_2$ resonances are clearly resolved and the relative amounts of PC and GPC can be easily quantified. The additional peaks at 4.095 and 3.96 ppm arise from other phosphorous containing brain metabolites such as, possibly, phosphoethanolamine (PE) and glycerophosphoethanolamine (GPE). [22] If these additional peaks prove to be due to PE and GPE, then the use of ^{31}P editing for quantification is even better justified. This is because the methyl signals of

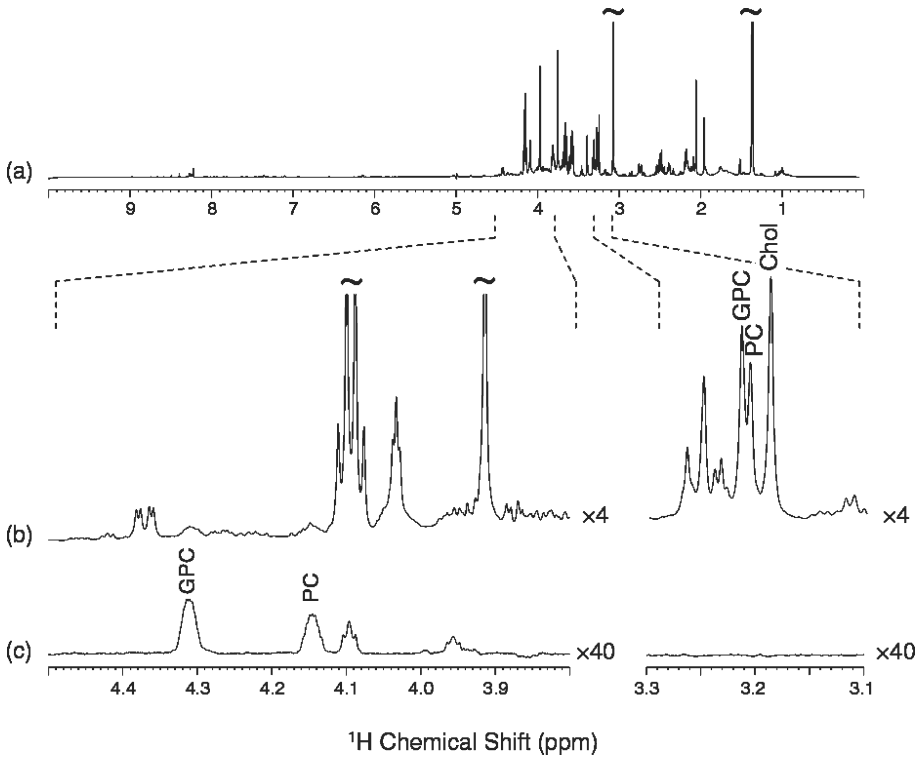

Figure 5. The 600 MHz regular (a) and ^{31}P edited ^{1}H (c) spectra obtained for a human glioma extract sample. Spectrum (b) highlights two regions of the regular spectrum with the scale increased by a factor of 4. The scale of the ^{31}P edited ^{1}H spectrum shown as spectrum (c) is increased by a factor of 40 relative to spectrum (a). Peaks other than those from PC and GPC in the ^{31}P edited ^{1}H spectrum arise from other phosphorous-containing brain metabolites in the sample

PE and GPE interfere with the quantification of the PC, GPC, and choline methyl peaks in regular ^{1}H spectra.[22] In contrast, the PE and GPE peaks that appear in the ^{31}P edited ^{1}H spectrum are well-resolved and, consequently, do not affect the quantification of the $^{1}CH_2$ resonances from PC and GPC.

The graphs shown in the bottom half of Fig. 4 demonstrate the correlation between the results of fitting the methyl peaks in the regular ^{1}H spectra (as has been done in the past) vs the results from the ^{31}P edited ^{1}H experiment. The variation seen in these graphs is not surprising owing to difficulties in quantifying the methyl peaks in the regular ^{1}H spectra. These difficulties are due to: (1) the lack of baseline resolution between the methyl peaks, and (2) the presence of other components that overlap the methyl peaks. These difficulties can be expected to be greatly exacerbated when using an instrument at lower field or in the analysis of *ex vivo* tissue samples.

DISCUSSION

^{31}P spectroscopy vs ^{31}P edited ^{1}H spectroscopy

As the ^{31}P resonances of PC and GPC differ from one another by $\sim$3.5 ppm, it could be argued that a better approach for the quantification of PC and GPC would be to directly observe the ^{31}P signal.[2,36–39] In fact, with the development and availability of high field MR imagers, it has been demonstrated recently that PC and GPC can be observed in *in vivo* ^{31}P spectroscopy at 7 T from a voxel size of 27 ml.[40] However, it may be better to utilize the improved sensitivity of ^{1}H nuclei for detection due to the higher magnetogyric ratio of ^{1}H, especially if an inverse geometry probehead is in use (as is often the case for *ex vivo* studies). This is clearly demonstrated in Fig. 3. The signal-to-noise ratio for the peaks in the ^{31}P edited ^{1}H spectrum [Fig. 3(b)] is roughly 10 times greater than the signal-to-noise ratio of the resonances in the ^{31}P spectrum [Fig. 3(c)] when the line broadening is optimized. The signal-to-noise ratio was calculated as the ratio of the PC or GPC peak intensity to the root-mean-square noise of a signal-less spectral region. As quantitative work usually makes use of integrals instead of intensities, the comparison of these techniques based on their signal-to-noise ratios underestimates the advantages of the ^{31}P-filtered ^{1}H experiment because the peaks in the ^{31}P spectrum are approximately 10 times narrower than the $^{1}CH_2$ peaks in the ^{31}P filtered ^{1}H spectrum. In addition, ^{31}P nuclei typically relax more slowly than ^{1}H nuclei, so ^{31}P edited ^{1}H spectra will have a further signal-to-noise advantage compared with ^{31}P spectra when comparing data acquired with the same amount of experiment time instead of the same number of scans.

Signal intensities in ^{31}P edited ^{1}H spectra

The use of a ^{31}P filter for editing in these experiments reduces the signal intensity due to the added restrictions to the coherence transfer pathway. In theory, the edited spectrum should have 50% of the intensity of the unedited spectrum if only phase cycling is used for selecting the coherence transfer pathway. However, we found that it was useful to supplement the phase cycling with pulsed field gradients to further attenuate artifacts in the spectrum. However, this comes at the price of an additional two-fold reduction in signal intensity, resulting in a total theoretical transfer efficiency of 25%.

INEPT transfer vs Hartman–Hahn mixing

We note that we also attempted to use heteronuclear Hartman–Hahn mixing[41] for the heteronuclear transfer steps. However, the measured transfer efficiency was around 3%, much lower than the efficiency of INEPT transfers. The inefficiency of heteronuclear Hartman–Hahn mixing compared with INEPT is attributable to the longer periods required to complete the heteronuclear magnetization transfer as well as to interference from homonuclear Hartman–Hahn mixing.

Realistic experiment times

The use of a non-quantitative extraction procedure for the preparation of the human glioma samples used in this study led to relatively low metabolite concentrations. Consequently, the ^{1}H spectra for the brain extracts were acquired using 1024 scans, resulting in an experiment time of 3.2 h, and the ^{31}P edited ^{1}H spectra were acquired using between 3096 and 5192 scans, resulting in quite lengthy experiment times of between 9.8 and 16.3 h. Owing to the low metabolite concentrations, as well as other factors, the measurement times used for these experiments are much longer than what will typically be needed. If samples were used with metabolite concentrations similar to those reported in the literature (which are about four times higher than the concentrations of the brain extract samples used for this study), then a spectrum equivalent to the results shown in Fig. 5 could be achieved while reducing the experiment time by a factor of 16. In addition, the signal-to-noise ratio (SNR) shown in Fig. 5 is greater than what is actually needed for quantification. If half the SNR were deemed acceptable for quantification, than the experiment time could be reduced by a factor of 4. Combined, these two changes would reduce the experiment time by a factor of 64, shortening a 9.8 h experiment to a much more reasonable 9.5 min experiment. In addition, experiment times can be further reduced by using shorter recycle delays as long as all samples are analyzed using the same conditions.

CONCLUSION

We have demonstrated a scheme that uses ^{31}P edited ^{1}H NMR spectroscopy to quantify the concentrations of phosphocholine and glycerophosphocholine in biological samples. In addition, the concentration of choline can be indirectly determined using this method. This method is particularly well-suited for analytical situations in which the $^{1}CH_2$ resonances are obscured by other metabolites and/or the methyl resonances are not sufficiently resolved. We believe this method will be applicable for the analysis of choline compounds in *ex vivo* tissue samples. In addition, if problems of sensitivity are resolved, this method may have potential for the *in vivo* non-destructive quantification of choline, PC and GPC.

Acknowledgements

The authors thank Prof*s*. Robert G. Griffin and Franca Podo for useful discussion and Dr. Anthony Bielecki for assistance. N.M.L. thanks the National Institutes of Health for support via a National Research Service Award post-doctoral fellowship (F32 NS42425-01) and the Camille and Henry Dreyfus Foundation for support through a Faculty Start-Up Award. This work is supported in part by NIH NCI grants CA77727, CA095624, CA83159, and by NIH NIBIB grant EB002026.

REFERENCES

1. Holmes HC, Snodgrass GJ, Iles RA. Changes in the choline content of human breast milk in the first 3 weeks after birth. *Eur. J. Pediatr.* 2000; **159**(3): 198–204.
2. Podo F. Tumour phospholipid metabolism. *NMR Biomed.* 1999; **12**(7): 413–439.
3. Chang L, Ernst T, Witt MD, Ames N, Walot I, Jovicich J, DeSilva M, Trivedi N, Speck O, Miller EN. Persistent brain abnormalities in antiretroviral-naive HIV patients 3 months after HAART. *Antivir. Ther.* 2003; **8**(1): 17–26.
4. Brenner T, Freier MC, Holshouser BA, Burley T, Ashwal S. Predicting neuropsychologic outcome after traumatic brain injury in children. *Pediatr. Neurol.* 2003; **28**(2): 104–114.
5. Delamillieure P, Constans JM, Fernandez J, Brazo P, Benali K, Courtheoux P, Thibaut F, Petit M, Dollfus S. Proton magnetic resonance spectroscopy (^{1}H MRS) in schizophrenia: investigation of the right and left hippocampus, thalamus, and prefrontal cortex. *Schizophr. Bull.* 2002; **28**(2): 329–339.
6. Firbank MJ, Harrison RM, O'Brien JT. A comprehensive review of proton magnetic resonance spectroscopy studies in dementia and Parkinson's disease. *Dement. Geriatr. Cogn. Disord.* 2002; **14**(2): 64–76.
7. Brockmann K, Dechent P, Meins M, Haupt M, Sperner J, Stephani U, Frahm J, Hanefeld F. Cerebral proton magnetic resonance spectroscopy in infantile Alexander disease. *J. Neurol.* 2003; **250**(3): 300–306.
8. Chaudhuri A, Condon BR, Gow JW, Brennan D, Hadley DM. Proton magnetic resonance spectroscopy of basal ganglia in chronic fatigue syndrome. *Neuroreport* 2003; **14**(2): 225–228.
9. Arnold DL, De Stefano N, Narayanan S, Matthews PM. Proton MR spectroscopy in multiple sclerosis. *Neuroimag. Clin. N. Am.* 2000; **10**(4): 789–798, ix–x.

10. Filippi CG, Ulug AM, Deck MD, Zimmerman RD, Heier LA. Developmental delay in children: assessment with proton MR spectroscopy. *AJNR Am. J. Neuroradiol.* 2002; **23**(5): 882–888.
11. Sijens PE, den Heijer T, Origgi D, Vermeer SE, Breteler MM, Hofman A, Oudkerk M. Brain changes with aging: MR spectroscopy at supraventricular plane shows differences between women and men. *Radiology* 2003; **226**(3): 889–896.
12. Galanaud D, Chinot O, Nicoli F, Confort-Gouny S, Le Fur Y, Barrie-Attarian M, Ranjeva JP, Fuentes S, Viout P, Figarella-Branger D, Cozzone PJ. Use of proton magnetic resonance spectroscopy of the brain to differentiate gliomatosis cerebri from low-grade glioma. *J. Neurosurg.* 2003; **98**(2): 269–276.
13. Rijpkema M, Schuuring J, Van Der Meulen Y, Van Der Graaf M, Bernsen H, Boerman R, Van Der Kogel A, Heerschap A. Characterization of oligodendrogliomas using short echo time ^{1}H MR spectroscopic imaging. *NMR Biomed.* 2003; **16**(1): 12–18.
14. Lindskog M, Kogner P, Ponthan F, Schweinhardt P, Sandstedt B, Heiden T, Helms G, Spenger C. Noninvasive estimation of tumour viability in a xenograft model of human neuroblastoma with proton magnetic resonance spectroscopy (^{1}H MRS). *Br. J. Cancer* 2003; **88**(3): 478–485.
15. Howe FA, Barton SJ, Cudlip SA, Stubbs M, Saunders DE, Murphy M, Wilkins P, Opstad KS, Doyle VL, McLean MA, Bell BA, Griffiths JR. Metabolic profiles of human brain tumors using quantitative *in vivo* ^{1}H magnetic resonance spectroscopy. *Magn. Reson. Med.* 2003; **49**(2): 223–232.
16. El-Sayed S, Bezabeh T, Odlum O, Patel R, Ahing S, MacDonald K, Somorjai RL, Smith IC. An *ex vivo* study exploring the diagnostic potential of ^{1}H magnetic resonance spectroscopy in squamous cell carcinoma of the head and neck region. *Head Neck* 2002; **24**(8): 766–772.
17. Katz-Brull R, Lavin PT, Lenkinski RE. Clinical utility of proton magnetic resonance spectroscopy in characterizing breast lesions. *J. Natl. Cancer Inst.* 2002; **94**(16): 1197–1203.
18. Nakagami K, Uchida T, Ohwada S, Koibuchi Y, Suda Y, Sekine T, Morishita Y. Increased choline kinase activity and elevated phosphocholine levels in human colon cancer. *Jpn. J. Cancer Res.* 1999; **90**(4): 419–424.
19. Sabatier J, Gilard V, Malet-Martino M, Ranjeva JP, Terral C, Breil S, Delisle MB, Manelfe C, Tremoulet M, Berry I. Characterization of choline compounds with *in vitro* ^{1}H magnetic resonance spectroscopy for the discrimination of primary brain tumors. *Invest. Radiol.* 1999; **34**(3): 230–235.
20. Morvan D, Demidem A, Papon J, De Latour M, Madelmont JC. Melanoma tumors acquire a new phospholipid metabolism phenotype under cystemustine as revealed by high-resolution magic angle spinning proton nuclear magnetic resonance spectroscopy of intact tumor samples. *Cancer Res.* 2002; **62**(6): 1890–1897.
21. Katz-Brull R, Margalit R, Degani H. Differential routing of choline in implanted breast cancer and normal organs. *Magn. Reson. Med.* 2001; **46**(1): 31–38.
22. Govindaraju V, Young K, Maudsley AA. Proton NMR chemical shifts and coupling constants for brain metabolites. *NMR Biomed.* 2000; **13**(3): 129–153.
23. Cheng LL, Ma MJ, Becerra L, Ptak T, Tracey I, Lackner A, Gonzalez RG. Quantitative neuropathology by high resolution magic angle spinning proton magnetic resonance spectroscopy. *Proc. Natl. Acad. Sci. USA* 1997; **94**(12): 6408–6413.
24. Sitter B, Sonnewald U, Spraul M, Fjosne HE, Gribbestad IS. High-resolution magic angle spinning MRS of breast cancer tissue. *NMR Biomed.* 2002; **15**(5): 327–337.
25. Ala-Korpela M, Posio P, Mattila S, Korhonen A, Williams SR. Absolute quantification of phospholipid metabolites in brain-tissue extracts by ^{1}H NMR spectroscopy. *J. Magn. Reson. B* 1996; **113**(2): 184–189.
26. Moreno A, Lopez LA, Fabra A, Arus C. ^{1}H MRS markers of tumour growth in intrasplenic tumours and liver metastasis induced by injection of HT-29 cells in nude mice spleen. *NMR Biomed.* 1998; **11**(3): 93–106.
27. Morvan D, Demidem A, Papon J, De Latour M, Madelmont JC. Melanoma tumors acquire a new phospholipid metabolism phenotype under cystemustine as revealed by high-resolution magic angle spinning proton nuclear magnetic resonance spectroscopy of intact tumor samples. *Cancer Res.* 2002; **62**(6): 1890–1897.
28. Morvan D, Demidem A, Papon J, Madelmont JC. Quantitative HRMAS proton total correlation spectroscopy applied to cultured melanoma cells treated by chloroethyl nitrosourea: demonstration of phospholipid metabolism alterations. *Magn. Reson. Med.* 2003; **49**(2): 241–248.
29. Morris GA, Freeman R. Enhancement of nuclear magnetic-resonance signals by polarization transfer. *J. Am. Chem. Soc.* 1979; **101**: 760–762.
30. Davis AL, Estcourt G, Keeler J, Laue ED, Titman JJ. Improvement of z filters and purging pulses by the use of zero-quantum dephasing in inhomogenous B_1 and B_0 fields. *J. Magn. Reson.* 1993; **A105**: 167–183.
31. Shaka AJ, Keeler J, Freeman R. Evaluation of a new broad-band decoupling sequence—Waltz-16. *J. Magn. Reson.* 1983; **53**: 313–340.
32. Le Belle JE, Harris NG, Williams SR, Bhakoo KK. A comparison of cell and tissue extraction techniques using high-resolution ^{1}H-NMR spectroscopy. *NMR Biomed.* 2002; **15**(1): 37–44.
33. Peeling J, Sutherland G. High-resolution ^{1}H NMR spectroscopy studies of extracts of human cerebral neoplasms. *Magn. Reson. Med.* 1992; **24**(1): 123–136.
34. Sutton L, Wehrli S, Gennarelli L, Wang Z, Zimmerman R, Bonner K, Rorke L. High-resolution ^{1}H-magnetic resonance spectroscopy of pediatric posterior fossa tumors *in vitro*. *J. Neurosurg.* 1994; **81**(3): 443–448.
35. Kinoshita Y, Yokota A. Absolute concentrations of metabolites in human brain tumors using *in vitro* proton magnetic resonance spectroscopy. *NMR Biomed.* 1997; **10**(1): 2–12.
36. Ronen SM, Leach MO. Imaging biochemistry: applications to breast cancer. *Breast. Cancer Res.* 2001; **3**(1): 36–40.
37. Leach MO, Verrill M, Glaholm J, Smith TA, Collins DJ, Payne GS, Sharp JC, Ronen SM, McCready VR, Powles TJ, Smith IE. Measurements of human breast cancer using magnetic resonance spectroscopy: a review of clinical measurements and a report of localized ^{31}P measurements of response to treatment. *NMR Biomed.* 1998; **11**(7): 314–340.
38. Bhujwalla ZM, Aboagye EO, Gillies RJ, Chacko VP, Mendola CE, Backer JM. Nm23-transfected MDA-MB-435 human breast carcinoma cells form tumors with altered phospholipid metabolism and pH: a ^{31}P nuclear magnetic resonance study *in vivo* and *in vitro*. *Magn. Reson. Med.* 1999; **41**(5): 897–903.
39. Lehtimaki KK, Valonen PK, Griffin JL, Vaisanen TH, Grohn OH, Kettunen MI, Vepsalainen J, Yla-Herttuala S, Nicholson J, Kauppinen RA. Metabolite changes in BT4C rat gliomas undergoing ganciclovir-thymidine kinase gene therapy-induced programmed cell death as studied by ^{1}H NMR spectroscopy *in vivo*, *ex vivo*, and *in vitro*. *J. Biol. Chem.* 2003; **278**(46): 45915–45923.
40. Lei H, Zhu XH, Zhang XL, Ugurbil K, Chen W. *In vivo* ^{31}P magnetic resonance spectroscopy of human brain at 7 T: an initial experience. *Magn. Reson. Med.* 2003; **49**(2): 199–205.
41. Ernst M, Griesinger C, Ernst RR. Optimized heteronuclear cross polarization in liquid. *Mol. Phys.* 1991; **74**: 219–252.

